CONF-800716--9

LA-UR 80-1680

90a

TITLE: MODELING AND INTERPRETATION OF TWO-PHASE FLOW AND TRACER STUDIES FROM A SUBBITUMINOUS COAL SEAM IN THE SAN JUAN BASIN OF NEW MEXICO

AUTHOR(s): H. E. Nuttall and B. J. Travis

MASTER

SUBMITTED TO: 6th Underground Coal Conversion Symposium

LOS ALAMOS SCIENTIFIC LABORATORY

MODELING AND INTERPRETATION OF TWO-PHASE FLOW AND TRACER STUDIES FROM A SUBBITUMINOUS COAL SEAM IN THE SAN JUAN BASIN OF NEW MEXICO

H. E. Nuttall
Dept. of Chemical Engineering
University of New Mexico
Albuquerque, NM 87131

B. J. Travis
Geosciences Division
Los Alamos Scientific Laboratory
Los Alamos, NM 87545

ABSTRACT

Field and modeling studies were performed to characterize two-phase flow within the natural cleat structure of an upper Cretaceous subbituminous coal seam. A two borehole pattern with open completion was used in a study of dewatering and tracer residence time distribution. Air was pumped into a five meter thick seam located about 170 meters below the surface. Krypton 85 was used as the airborne tracer. Air inflow and air and water production rates and tracer arrival times were monitored. The field tests were simulated with a two-phase three component porous flow code. Results showed that the air inflow and air and water outflow rates and breakthrough times could not be modeled assuming a uniform darcy-type permeability. The use of a pressure dependent permeability did provide, however, a much better match with the field data.

NOMENCLATURE

$a_{I,II}$	geometric dispersivity (cm)
C_α	concentration of component α (gm/gm)
C_m	thermal conductivity of matrix (ergs/cm·s·cm^3)
D_{ij}	components of dispersion tensor (cm^2/s)
$\vec{D}_g$	diffusion vector for gas
$\vec{D}_v$	diffusion vector for vapor
$D^*_{\alpha\gamma}$	molecular diffusivity of component α in phase γ
E_f	fluid energy density (ergs/cm^3)
E_m	matrix energy density (ergs/cm^3)
$\dot{E}_f$	energy source/sink rate for fluid energy (ergs/s·cm^3)
$\dot{E}_m$	energy source/sink rate for matrix (ergs/s·cm^3)
f	gas saturation
$\vec{g}$	gravity (cm/s^2)
H_i	enthalpy of phase i (ergs/cm^3)
k_i	effective permeability for phase i (darcy)
M_{ij}	coordinate system metric
P_i	pressure in phase i (dynes/cm^2)
Pe	Peclet number
Re_i	Reynolds number for phase i
$\dot{S}_g$	mass source/sink rate for noncondensable gas (gm/s·cm^3)
$\dot{S}_{\ell v}$	mass source/sink rate for condensable component (gm/s·cm^3)
t	time (s)
T_f	fluid temperature (°C)
T_m	matrix temperature (°C)
$\vec{v}$	velocity (cm/s)
β	heat exchange coefficient (ergs/°C·cm^3)
δ	channel shape parameter
ϵ	porosity
μ_i	viscosity of phase i (gm/cm·s)
ρ_i	density of phase i (gm/cm^3)
σ	water saturation
g	subscript referring to noncondensable gas
gv	subscript referring to gas and vapor mixture
i	subscript for phase i
ℓ	subscript referring to liquid condition
v	subscript referring to vapor

INTRODUCTION

A primary technical requirement for the operation of underground coal gasification and most other in situ technologies is the ability to create and to maintain an optimal flow pattern within the desired processing region. Many approaches have been tried in an effort to engineer and thus control the flow of the working fluid through the geomedium. These include rubblization, fracturing, and various linking methods. A first and essential step in initiating and subsequently maintaining desired flow patterns in a geomedium is to know something about the naturally occurring flow paths and behavior of the proposed working region. Only recently, in the latest Hanna field experiments, did this need to know the flow characteristics of the coal formation become clearly demonstrated. A local fracture in the coal seam prevented the formation of a normal flow pattern and adversely affected the subsequent burn at that site. Other problems in flow control, such as override, have occurred at underground coal conversion (UCC) tests in both Texas[1] and Wyoming.[2-4].

Experience to this point has shown that the flow pattern within the formation is a key factor to the success of UCC[4] and that the development work to date has not solved this important design problem. The work described in this paper is a beginning effort to more fully understand and characterize the preburn flow structure of a subbituminous coal by the use of air acceptance, dewatering, and tracer studies.

Several attempts at studying flow within coal have been undertaken. Interest in the natural flow structure of a coal formation has been limited to cases where a highly permeable zone surrounded the coal seam. As was demonstrated by the recent Hanna IV test experience,[4] a thorough knowledge of the natural flow environment is extremely important since faults and highly permeable zones will affect the subsequent processing steps. Prior to this work, preburn studies on the flow structure of a coal seam have been limited primarily to hydrology tests that can only give area averaged flow conditions and a general indication of directional permeability, whereas detailed information, indicating, e.g., faults and highly permeable zones, is probably not detected. Modeling studies of the natural flow and dewatering process has also been limited. Strickland and Jennings[5] modeled the problem of a highly permeable water sand zone above and below the coal. They used a two-dimensional (r - z), two-phase (air/water), finite difference numerical simulator to simulate the effects of the highly permeable sand formation. The results showed how the air bypassed the coal seam and followed the more permeable sand formation. Their simulation was for a single well and did not show the effects of a production well. Also, no tracer studies were performed at their site.

In general, the use of tracers[6] has been limited to studying the coal seam following some type of disturbance to the formation, i.e., after fracturing, during reverse linking, or forward gasification. Tracer studies have shown their versatility during UCC burns at Hoe Creek[2] and Hanna.[4] A tracer has been used to investigate the growth of the burn cavity and the nature of the link during reverse combustion. The model interpretation of the data was limited to either simple arrival time and active void volume determination or steady state two-dimensional, single-phase modeling.

Previous studies have not investigated in detail the preburn, two-phase flow characteristics within a coal seam. In the present investigation of underground coal conversion (UCC) in New Mexico, an integrated program has been followed in determining the suitability of UCC in this region.

UCC STUDIES IN NEW MEXICO

The study of UCC in the San Juan Basin of New Mexico began in 1977 with laboratory investigations[7] of the coal. These tests indicated that the San Juan, Fruitland formation contained a shrinking subbituminous coal that is very similar chemically to the Hanna, Wyoming, coal where successful UCC tests have been performed. Subsequent studies in New Mexico have focused on a detailed characterization of the geochemical and geophysical properties of a proposed UCC site[8-10] located in the northwest corner of the basin, about 15 miles west of Farmington, New Mexico, and directly east of the San Juan Generating Station.

The present study is a modeling analysis with field verification of the preburn two phase flow characteristics within the five-meter coal seam at the San Juan UCC test site. A two-hole pattern was drilled, then cored and cemented, as shown in Fig. 1. Open completion was made in the coal. Air acceptance and tracer tests were performed in July, 1979. A description of the geology and hydrology of the site was presented by Nuttall et al,[8] and the results of the current field test were given by Williams and Nuttall.[11]

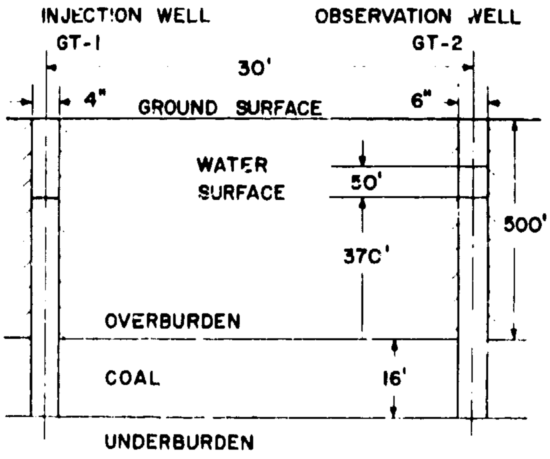

SAN JUAN UCC TEST SITE GEOMETRY
FIGURE 1

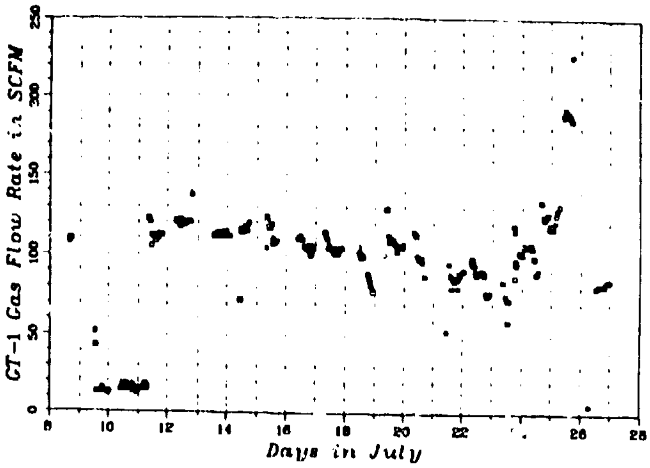

GAS INFLOW RATE AT GT-1
FIGURE 2

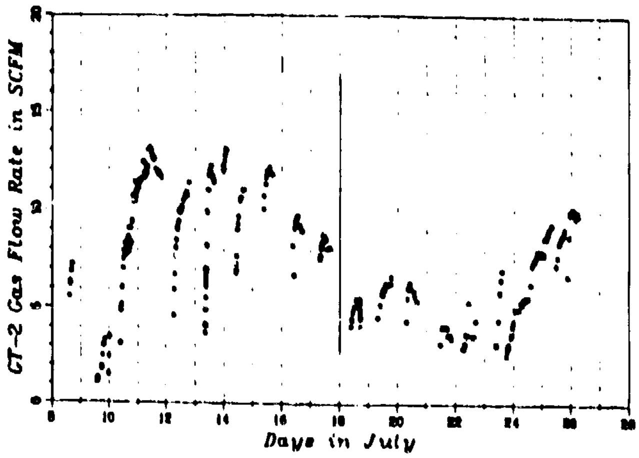

GAS OUTFLOW RATES AT GT-2
FIGURE 3

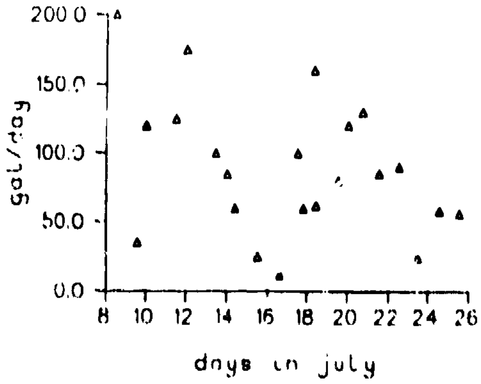

WATER OUTFLOW RATES AT GT-2
FIGURE 4

The objectives of the modeling and field study were to characterize the natural flow paths within the coal seam. The process of air acceptance, dewatering, and tracer injection was simulated, using an advanced two-phase geomedia transport code. Field data consisting of air in flow rates, water and air production rates, and tracer curves were compared to the model predictions. Results suggest that the air flow was primarily through cleats or joints within the coal and that the composite of field data can be interpreted by assuming a pressure dependent permeability within the seam.

A description of the model and an analysis of the field test data are presented in the following sections.

MODEL DESCRIPTION

Computer simulations described in this paper were made with a multidimensional, three-component, two-phase mass and heat transport model called WAFE.[12] Although the applications in this study do not exercise the full capabilities of the model, we nevertheless will give a complete (but brief) description of WAFE.

The WAFE model consists of conservation equations of mass, momentum and energy, and equations of state and constitutive relations, e.g., for effective permeability. In a non-reacting system each molecular species must be conserved. WAFE allows three components: a noncondensable gas, H_2O (liquid and vapor) and a tracer gas. The mass conservation equations for these are

gas
$$\epsilon \frac{\partial(f\rho_g)}{\partial t} + \nabla\cdot(\epsilon\rho_g \vec{V}_{gv}) = \epsilon \dot{S}_g + \nabla\cdot\vec{D}_g \quad (1)$$

H_2O
$$\epsilon \frac{\partial(f\rho_v + \epsilon\rho_\ell)}{\partial t} + \nabla\cdot\epsilon(\rho_v \vec{V}_{gv} + \rho_\ell \vec{V}_\ell) = \epsilon \dot{S}_{\ell v} + \nabla\cdot\vec{D}_v \quad (2)$$

tracer
$$\epsilon \frac{\partial(\rho_i C_\alpha)}{\partial t} + \nabla\cdot(\epsilon\rho_i C_\alpha \vec{V}_i) = \epsilon \dot{S}_\alpha + \nabla\cdot[\epsilon(\rho_i D^*_{\alpha\gamma} \nabla C_\alpha + D\nabla(\rho_i C_\alpha))] \quad (3)$$

The last term of (3) includes both molecular diffusion and mechanical dispersion. Dispersion is represented in full tensor form

$$D_{ij} = \left(\alpha_{TT} V \delta_{ij} + (\alpha_L - \alpha_{TT}) \frac{V_i V_j}{V}\right) q(P_e, \delta) \quad (4)$$

where the function q is that given by Bear.[13] The tracer gas can exist in either phase but at present cannot move from one phase to the other.

WAFE solves two energy equations, one for the fluid and another for the matrix. When flow rates are large and/or matrix particles are large, fluid and matrix will not necessarily be in thermodynamic equilibrium.

fluid
$$\epsilon \frac{\partial E_f}{\partial t} + \nabla\cdot\epsilon(h_{gv} \vec{V}_{gv} + h_\ell \vec{V}_\ell) = \epsilon \dot{\mathcal{E}}_f - \beta(T_f - T_m) + \nabla\cdot\vec{D}_{gv} \quad (5)$$

matrix
$$(1-\epsilon) \frac{\partial E_m}{\partial t} = \nabla\cdot C\,\nabla T_m + \beta(T_f - T_m) + (1-\epsilon)\,\dot{\mathcal{E}}_m \quad (6)$$

The term $\beta(T_f - T_m)$ represents heat transfer between fluid and "average" matrix grains.

In a porous medium, for low to moderate flow rates, the momentum conservation equations can be approximated by expressions of the Forchheimer type

$$(1 + a\,Re_i)\,\vec{V}_i = -\frac{k_i}{\epsilon\mu_i}(\nabla P_i + \rho_i \vec{g}) \quad (7)$$

At low Reynolds number, (7) reduces to Darcy's law. At higher Reynolds number (1-100), nonlinear effects become important and (7) is much more accurate than a simple Darcy formulation.

To complete the model, equations of state and certain constitutive relations are needed. The noncondensable component is treated as a perfect gas and tables are used for the thermodynamic properties of H_2O, liquid and vapor. Effective permeability for each phase depends on phase saturation, capillary pressure and pressure gradients. Fluid viscosities are strongly temperature dependent. Derivation of equations 1-7 for porous media can be found in Reference 13.

WAFE solves equations 1-7 plus equations of state in Cartesian or cylindrical geometry using a finite difference control volume numerical technique. Material properties can vary spatially and a variety of boundary conditions are available. The code is flexible in that it can run transient, one- or two-dimensional problems (3-D is available for tracer flow alone[14]), using one, two, or three components under isothermal or non-isothermal conditions for one- or two-phase flow.

COMPUTER SIMULATIONS

The flow model described in the

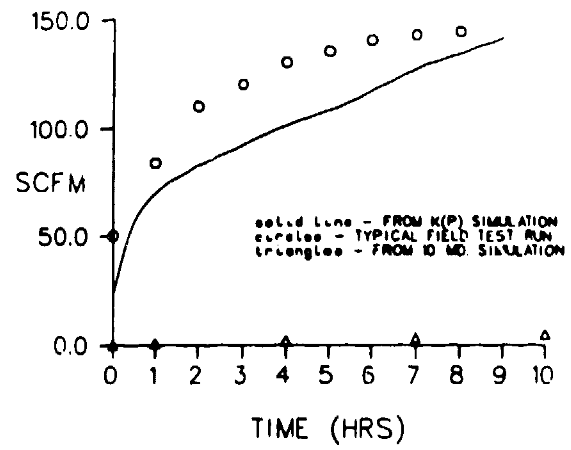

AIR INFLOW AT GT-1, AS CALCULATED AND
AS OBSERVED ON A TYPICAL FIELD RUN
FIGURE 5

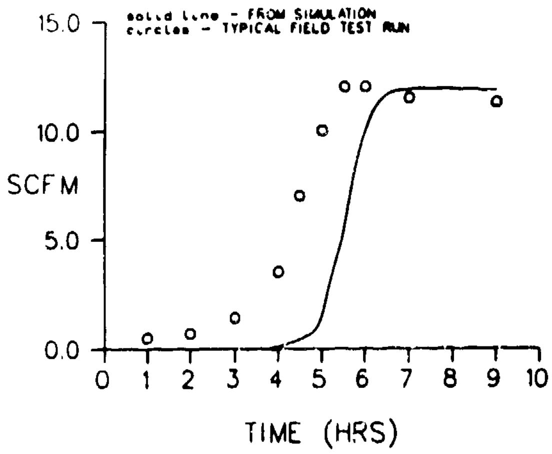

AIR OUTFLOW AT GT-2, AS CALCULATED
AND AS OBSERVED. EARLY PRODUCTION
AT LOW RATES WITH LATER ARRIVAL OF
BULK OF FLOW SUGGESTS PRESENCE OF A
FEW OPEN CRACKS IN A NETWORK OF MUCH
NARROWER FRACTURES AND PORES.
FIGURE 6

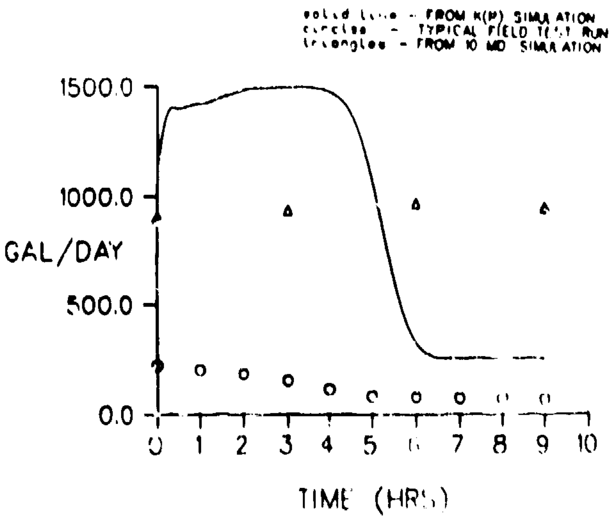

WATER OUTFLOW AT GT-2, AS
CALCULATED AND AS OBSERVED.
FIGURE 7

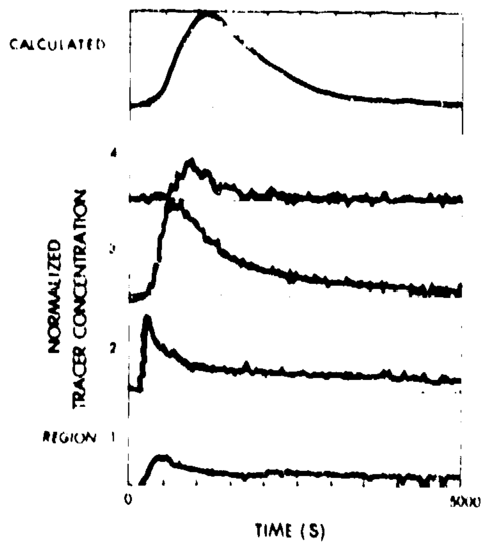

TRACER CONCENTRATION HISTORIES AS
MEASURED AT FOUR LEVELS IN GT-2
AND AS CALCULATED.
FIGURE 8

preceding section was used to simulate the field tests. The air injection tests were carried out over a period of about a month (July, 1979). The time history is complex-- the air pumps were turned on for several hours, up to a day, then shut off. This on-off pattern was repeated many times. The resulting injection and production rates were, however, very reproducible as seen in Figures 2-4. Pressure in the injection hole, labeled GT-1, was maintained near 250 psia (1.725 MPa) during pumping. This pressure varied by as much as 10% during some runs. In the computer simulations, the source, GT-1, was idealized to an air-filled cylinder maintained at a constant pressure of 250 psia. (1.725 MPa).

Porosity of Fruitland coal is approximately 10%. The in situ permeability as determined from a drawdown test at the site is 10 millidarcies. Capillary pressure effects were ignored because of lack of data. The coal seam is below the water table and was initially fully saturated. The immobile water fraction, S_{wi}, for this material is unknown; we made calculations for 0% S_{wi}.

For the simulations, a planar geometry was used to show flow in a plane in the coal seam perpendicular to the boreholes. Variations in flow with depth are ignored here. (Buoyancy effects, resulting in over-ride, can be significant, especially as hole separation increases. Three-dimensional calculations for a single well in cylindrical geometry with axisymmetry using the WAFE model clearly show the increasing importance of over-ride with distance from the air source. Three-dimensional calculations for a two-hole pattern showing effect of buoyancy will be the subject of a future paper.) In the vicinity of GT-1 and GT-2, the overburden and underburden materials have much lower permeability than the coal seam, an ideal situation. The computational outer boundaries were kept at constant pressure (180 psia, the far field ambient pressure) and were placed at a large distance from the boreholes.

The first simulation used a constant 10 md. permeability. The resulting air injection and air and water production rates were an order of magnitude off from the observations and the breakthrough time was several days rather than several hours. Clearly, the assumption of a constant 10 md. permeability is seriously in error. We decided to try a pressure dependent permeability which increased linearly from 10 md. at ambient pressure to 1. darcy at 250 psia. At pressures below ambient (180 psia), the permeability was left at 10 md. If air and water flow is predominantly through a fracture network, internal pressurization would tend to open up the fractures, greatly increasing their effective permeability.

The simulation using pressure dependent permeability gave much better agreement with observations (see Figures 5-7). Air inflow rate at GT-1 rises rapidly for about an hour, then at a slower, more or less constant rate; the air inflow is on the order of 100 SCFM which is typical of the field conditions. Air production at GT-2 begins a few hours after start up, rises rapidly and levels off around 12 SCFM, in very good agreement with the data. Breakthrough occurs at GT-2 after about five hours, which is somewhat later than observed. Water production at GT-2 as calculated by the model is too large. Water outflow decreases from a maximum of about 1500 gal/day to a steady rate of about 250 gal/day. In the field water production at GT-2 ranged from an initial high of several hundred gal/day down to 50-100 gal/day. Near the end of the field testing period, a tracer gas (^{85}Kr) flow test was carried out. Injection occurred in GT-1; GT-2 was packed off into four monitoring levels. Tracer concentration histories for each level are shown in Figure 8. Inflow rates were not uniform for the four levels; the uppermost quadrant received at about twice the rate seen in the lower sections. The tracer test was simulated with the flow model. The calculated concentration history at GT-2 is also shown in Figure 8. Qualitatively the curves are very similar-- a rapid rise to the maximum and then a gradual decline as tracer particles that took more tortuous paths through the coal arrive at GT-2.

The qualitative differences in flow between the small, constant permeability case and the pressure dependent permeability case are illustrated in Figures 9-12. These show pressure and water saturation contours for the two simulations at selected times. (Only half of the coal seam is shown because of symmetry about the line joining GT-1 and GT-2.) GT-2 has a strong effect on the flow in the 10 md. permeability case, whereas its influence on the pressure dependent permeability case is highly localized.

This calculational study is not complete. There are still a number of factors to be considered which may lead to a more accurate description of the flow characteristics of this coal seam. The calculations indicate small pressure gradients in the coal. Under this circumstance, capillary pressure (ignored here) may have a significant retarding effect on water

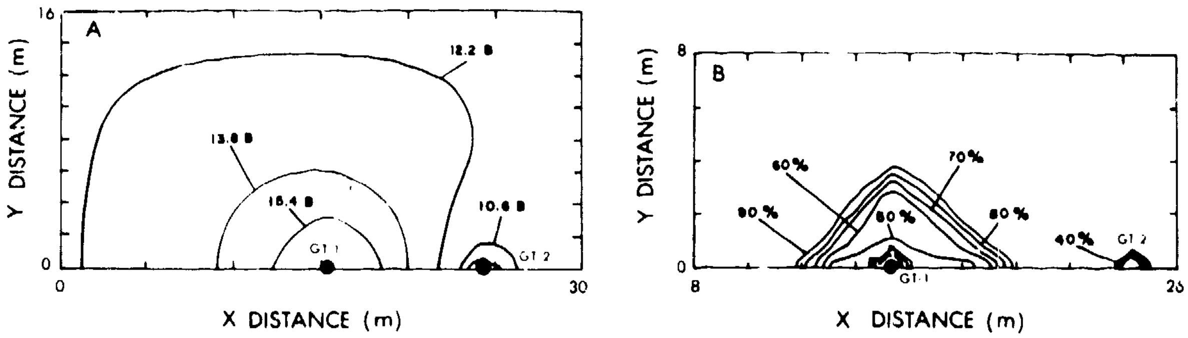

PRESSURE (A) AND WATER SATURATION (B) ISOLINES AT 1.5 DAYS. CONSTANT 10 MD. PERMEABILITY CASE. PRESSURE IN BARS. GT-2 HAS SIGNIFICANT INFLUENCE ON PRESSURE DISTRIBUTION.

FIGURE 9

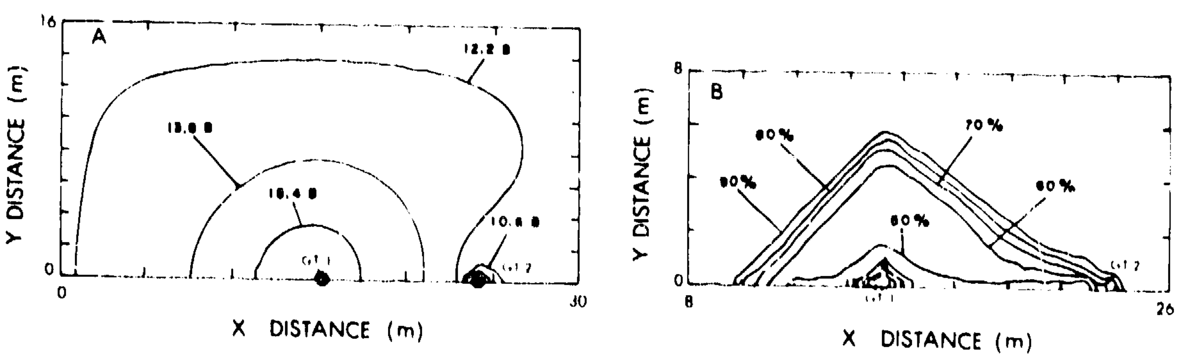

PRESSURE (A) AND WATER SATURATION (B) ISOLINES AT 3.0 DAYS. CONSTANT 10 MD. PERMEABILITY CASE. PRESSURE IN BARS. AIR FLOW IS CHANNELING INTO GT-2.

FIGURE 10

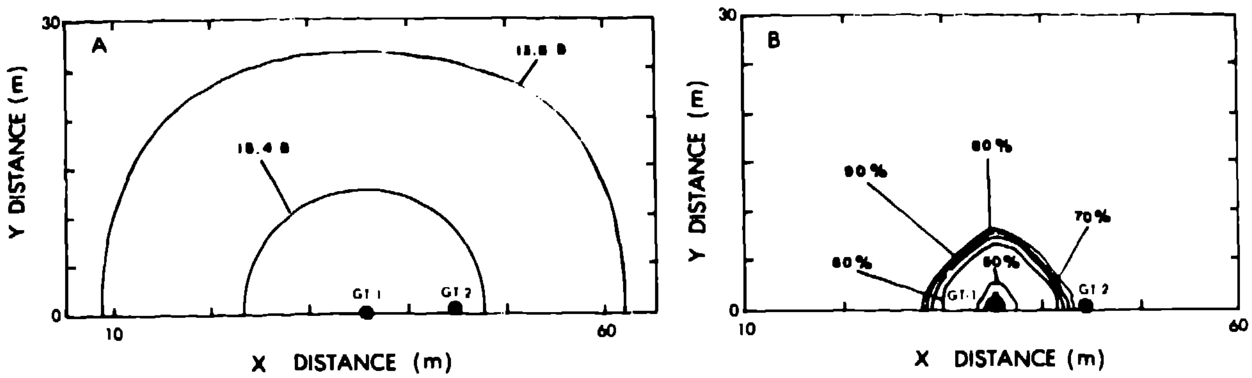

PRESSURE (A) AND WATER SATURATION (B) ISOLINES AT 4 HOURS. PRESSURE DEPENDENT PERMEABILITY CASE. PRESSURE IN BARS. PRESENCE OF GT-2 HAS VERY LITTLE EFFECT ON FAR-FIELD FLOW PATTERN.

FIGURE 11

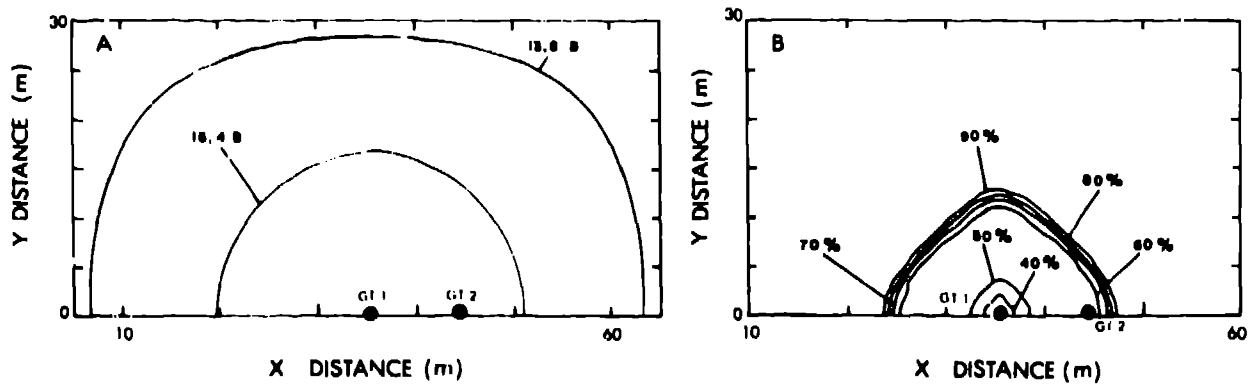

PRESSURE (A) AND WATER SATURATION (B) ISOLINES AT 8 HOURS. PRESSURE DEPENDENT PERMEABILITY CASE. PRESSURE IN BARS. EFFECT OF GT-2 ON FLOW PATTERN IS HIGHLY LOCALIZED.

FIGURE 12

flow. Also, the immobile water fraction and buoyancy effects can alter flow patterns and rates. There are also other data sets from this field experiment that have not been analyzed, such as decompression tests. Finally, the intermittent nature of the field tests may be informative. Additional tests, involving four or five hole patterns, are planned for the near future.

ACKNOWLEDGMENTS

The authors wish to recognize the support provided by the U. S. Department of Energy, the Public Service Company of New Mexico and Western Coal Company. Special appreciation is extended to the Los Alamos Scientific Laboratory for providing computer facilities and for secretarial support in preparing this paper.

REFERENCES

1. A. A. Reznik, Cheng-Li Lien, and P. F. Fulton, "Permeability Characteristics of Coal," Proceedings of the 4th Underground Coal Conversion Symposium, Steamboat Springs, Colorado, July 17-20, 1978, pp. 435-451.

2. R. W. Lyczkowsky, C. B. Thorsness, and R. J. Cena, "The Use of Tracers in Laboratory and Field Tests of Underground Coal Gasification and Oil Shale Retorting," Proceedings of the 4th Underground Coal Conversion Symposium, Steamboat Springs, Colorado, July 17-20, 1978.

3. R. W. Hill, C. B. Thorsness, D. R. Stephens, D. S. Thompson, and W. R. Aiman, "The LLL Underground Coal Gasification Project: 1978 Status," Proceedings of the 4th Underground Coal Conversion Symposium, Steamboat Springs, Colorado, July 17-20, 1978, pp. 19-40.

4. T. C. Bartke, L. Dookter, T. E. Sterner, J. E. Virgona, and L. F. Wojdac, "Status Report on the Hanna III and Hanna IV Underground Coal Gasification Experiments," Proceedings of the 4th Underground Coal Conversion Symposium, Steamboat Springs, Colorado, July 17-20, 1978, pp. 41-49.

5. R. F. Strickland and J. W. Jennings, "Recent Developments in Texas A and M University's Lignite Gasification Project," Proceedings of the 4th Underground Coal Conversion Symposium, Steamboat Springs, Colorado, July 17-20, 1978.

6. P. F. Ahner and R. F. Gensen, "Helium Tracer Studies to Characterize Underground Flow Paths," Proceedings of the 5th Underground Coal Conversion Symposium, Steamboat Springs, Colorado, June 18-21, 1979, pp. 199-211.

7. H. E. Nuttall and E. A. Walters, "In Situ Gasification of New Mexico's Deep Seam Coal Deposits Via Non-Mining Techniques," Report No. NE-37(77) BEF-363-1, Bureau of Engineering Research, University of New Mexico, April 1977.

8. H. E. Nuttall, E. A. Walters, and T. M. Niemctyk, "Hydrologic and Environmental Findings: San Juan UCC Site," Proceedings of the 5th Underground Coal Conversion Symposium, June 18-21, 1979, pp. 275-280.

9. H. E. Nuttall and C. Anderson, "A Field and Laboratory Project to Assess the Technical Suitability of New Mexico's Deep Seam San Juan Coal for In Situ Coal Gasification," Proceedings of the 4th Underground Coal Conversion Symposium, July 17-20, 1978, pp. 115-122.

10. H. E. Nuttall, "Suitability of New Mexico's Deep Seam San Juan Coal for In Situ Coal Gasification: Field and Laboratory Assessment," Final Report No. NE-62(79) PNM-162-0, Bureau of Engineering Research, University of New Mexico, 1979.

11. F. L. Williams and H. E. Nuttall, "Trace and Air Acceptance Characterization of a Subbituminous Coal Seam Located in the San Juan Basin of New Mexico," Proceedings of the 6th Annual Underground Coal Conversion Symposium, July 1980.

12. B. J. Travis, "Calculation of Two-Phase, Three-Component Mass and Heat Transport in Porous Media Using the WAFE Code," LA Report, in preparation.

13. J. Bear, Dynamics of Fluids in Porous Media, (American Elsevier, New York, 1972), Chapters 4 and 10.

14. B. J. Travis, "TRACR3D: A Computer Code for Calculating Three-Dimensional Flow of a Tracer Gas in a Porous Medium," LA Report, in preparation.